Three Dimensional Object Modeling via Minimal Surfaces

Vicent Caselles[1], Ron Kimmel[2], Guillermo Sapiro[3], and Catalina Sbert[1]

[1] Dept. of Mathematics and Informatics, University of Illes Balears, 07071 Palma de Mallorca, Spain
[2] Mail-stop 50A-2129, LBL, UC Berkeley, CA 94720, USA
[3] Hewlett-Packard Labs, 1501 Page Mill Road, Palo Alto, CA 94304

Abstract. A novel geometric approach for $3D$ object segmentation and representation is presented. The scheme is based on geometric deformable surfaces moving towards the objects to be detected. We show that this model is equivalent to the computation of surfaces of minimal area, better known as 'minimal surfaces,' in a Riemannian space. This space is defined by a metric induced from the $3D$ image (volumetric data) in which the objects are to be detected. The model shows the relation between classical deformable surfaces obtained via energy minimization, and geometric ones derived from curvature based flows. The new approach is stable, robust, and automatically handles changes in the surface topology during the deformation. Based on an efficient numerical algorithm for surface evolution, we present examples of object detection in real and synthetic images.

1 Introduction

One of the basic problems in image analysis is object detection. This can be associated with the problem of boundary detection, when boundary is roughly defined as a curve or surface separating homogeneous regions. "Snakes," or active contours, were proposed by Kass *et al.* in [17] to solve this problem, and were later extended to $3D$ surfaces. The classical snakes and $3D$ deformable surfaces approach are based on deforming an initial contour or surface towards the boundary of the object to be detected. The deformation is obtained by minimizing a functional designed such that its (local) minima is obtained at the boundary of the object [3, 36]. The energy usually involves two terms, one controlling the smoothness of the surface and another one attracting it to the boundary. These energy models are not capable of changing its topology when direct implementations are performed. The topology of the final surface will in general be as that of the initial one, unless special procedures are used for detecting possible splitting and merging [24, 34]. This approach is also non intrinsic, i.e., the energy functional depends on the parameterization. See for example [23, 39] for comments on advantages and disadvantages of energy approaches for deforming surfaces.

Recently, geometric models of deformable contours/surfaces were simultaneously proposed by Caselles *et al.* [4] and by Malladi *et al.* [23]. In these models,

the curve/surface is propagating by an implicit velocity that also contains two terms, one related to the regularity of the deforming shape and the other attracting it to the boundary. The model is given by a geometric flow (PDE), based on mean curvature motion, and is not a result of minimizing an energy functional. This model automatically handles changes in topology when implemented using the level-sets numerical algorithm [26]. Thereby, several objects can be detected simultaneously, without previous knowledge of their exact number in the scene, and without special tracking procedures.

In [5], we have shown the formal mathematical relation between these two approaches for $2D$ object detection. We also extended them proposing what we named "geodesic active contours." The geodesic active contours model has the following main properties: 1- It connects energy and curve evolution approaches of active contours. 2- Presents the snake problem as a geodesic computation one. 3- Improves existing models as a result of the geodesic formulation. 4- Allows simultaneous detection of interior and exterior boundaries of several objects without special contour tracking procedures. 5- Holds formal existence, uniqueness, and stability results. 6- Stops automatically.

In this paper we extend the results in [5] to $3D$ object detection. The obtained geometric flow is based on geometric deformable surfaces. We show that the desired boundary is given by a minimal surface in a Riemannian space defined by the image. In other words, segmentation is achieved via the computation of surfaces of minimal area, where the area is defined in a non-Euclidean space. The obtained flow has the same advantages over other $3D$ deformable models, similar to the advantages of the geodesic active contours over previous $2D$ approaches.

We note that the deformable surfaces model is related to a number of previously or simultaneously developed results. It is of course closely related to the works of Terzopoulos and colleagues on energy based deformable surfaces, and the works by Caselles *et al.* and Malladi *et al.* [4, 23]. It is an extension of the $2D$ model derived in [5]. The basic equations in this paper, as well as the corresponding $2D$ ones in [5], were simultaneously developed in [18, 33]. Similar $3D$ models are studied in [37, 38] as well. Extensions to [4, 23] are presented also in [35]. The similitude and differences with those approaches will be presented after describing the basic principles of the model.

2 Energy and Geometry based approaches of deformable surfaces

The $3D$ extension of the $2D$ snakes, known as the deformable surface model, was introduced by Terzopoulos *et al.* [36]. It was extended for $3D$ segmentation by many others (e.g. [9, 10, 11]). In the $3D$ case, a parameterized surface $v(r,s) = (x(r,s), y(r,s), z(r,s)) \quad (r,s) \in [0,1] \times [0,1]$, is considered, and the energy functional is given by

$$E(v) = \int_\Omega \left[\omega_{10} \left| \frac{\partial v}{\partial r} \right|^2 + \omega_{01} \left| \frac{\partial v}{\partial s} \right|^2 + \omega_{11} \left| \frac{\partial^2 v}{\partial r \partial s} \right|^2 + \omega_{20} \left| \frac{\partial^2 v}{\partial r^2} \right|^2 + \omega_{02} \left| \frac{\partial^2 v}{\partial s^2} \right|^2 + P \right] dr ds,$$

where $P := - \| \nabla I \|^2$, or any related decreasing function of the gradient, where I is the image. The first terms are related to the smoothness of the surface, while

the last one is responsible of attracting it to the object. The algorithm starts with an initial surface $\mathcal{S}_0$, generally near the desired $3D$ boundary O, and tries to move $\mathcal{S}_0$ towards a local minimum of E.

The geometric models proposed in [4, 23] can easily be extended to $3D$ object detection. Let $Q =: [0,a] \times [0,b] \times [0,c]$ and $I : Q \rightarrow \mathbb{R}^+$ be a given $3D$ data image. Let $g(I) = 1/(1+|\nabla \hat{I}|^p)$, where $\hat{I}$ a regularized version of I, and $p = 1$ or 2. $g(I)$ acts as an edge detector so that the object we are looking for is ideally given by the equation $g = 0$. Our initial active surface $\mathcal{S}_0$ will be embedded as a level set of a function $u_0 : Q \rightarrow \mathbb{R}^+$, say $\mathcal{S}_0 = \{x : u_0(x) = 0\}$ with u_0 being positive in the exterior and negative in the interior of $\mathcal{S}_0$. The evolving active surface is defined by $\mathcal{S}_t = \{x : u(t,x) = 0\}$ where $u(t,x)$ is the solution of

$$\frac{\partial u}{\partial t} = g(I)|\nabla u|\mathrm{div}\left(\frac{\nabla u}{|\nabla u|}\right) + \nu g(I)|\nabla u| = g(I)(\nu + \mathbf{H})|\nabla u|, \qquad (1)$$

with initial condition $u(0,x) = u_0(x)$ and Neumann boundary conditions. Here $\mathbf{H} = \mathrm{div}\left(\frac{\nabla u}{|\nabla u|}\right)$ is the sum of the two principal curvatures of the level sets $\mathcal{S}$ (twice its mean curvature,) and ν is a positive real constant. The $2D$ version of this model was heuristically justified in [4, 23]. It contains: 1. A smoothing term: Twice the mean curvature in the case of (1). More efficient smoothing velocities as those proposed in [2, 7, 25] can be used instead of $\mathbf{H}$.[4]. 2. A constant balloon-type force ($\nu|\nabla u|$). 3. A stopping factor ($g(I)$). The sign conventions here are adapted to inwards propagating active contours. For active contours evolving from the inside outwards, we take $\nu < 0$. This is a drawback of this model: the active contours cannot go in both directions (see also [35]). Moreover, we always need to select $\nu \neq 0$ even if the surface is close to the object's boundary.

Our goal will be to define a $3D$ geometric model (with level set formulation) corresponding the minimization of a meaningful and intrinsic energy functional. It is motivated by the extension of $2D$ geometric model to the geodesic active contours as done in [5].

3 Three dimensional deformable models as minimal surfaces

In [5], a model for $2D$ object detection based on the computation of geodesics in a given Riemannian space was presented. This means that we are computing paths or curves of minimal (weighted) length. This idea may be extended to $3D$ surfaces by computing surfaces of minimal area, where the area is defined in a given Riemannian space. In the case of surfaces, arc length is replaced by surface area $A := \int\int da$, and weighted arc length by "weighted" area

$$A_R := \int\int g(I)da, \qquad (2)$$

[4] Although curvature flows smooth $2D$ curves [15, 16, 30, 31], a $3D$ geometric flow that smoothes all possible surfaces was not found [25]. Frequently used are mean curvature or the positive part of the Gaussian curvature flows [2, 7].

where da is the (Euclidean) element of area. Surfaces minimizing A are denoted as *minimal surfaces* [27]. In the same manner, we will denote by minimal surfaces those surfaces that minimize (2). The area element da is given by the classical area element in Euclidean space, while the area element da_r is given by $g(I)da$. Observe that da_r corresponds to the area element induced on a surface of $\mathbb{R}^3$ by the metric of $\mathbb{R}^3$ given by $g_{ij}\,dx_i dx_j$ with $g_{ij} = g(I)^2\delta_{ij}$. This is the $3D$ analogue of the metric used in [5] to construct the geodesic active contour model. The energy A_R can be formally derived from the original energy formulation using basic principles of dynamical systems [5], further justifying this model. The basic element of our deformable model will be given by minimizing (2) by means of an evolution equation obtained from its Euler-Lagrange. Let us point out the basic characteristics of this flow.

The Euler-Lagrange of A is given by the mean curvature $\mathbf{H}$, resulting a curvature (steepest descent) flow $\frac{\partial \mathcal{S}}{\partial t} = \mathbf{H}\mathcal{N}$, where $\mathcal{S}$ is the $3D$ surface and $\mathcal{N}$ its inner unit normal. With the sign conventions explained above, the corresponding level set [26] formulation is $u_t = |\nabla u|\mathrm{div}\left(\frac{\nabla u}{|\nabla u|}\right) = |\nabla u|\mathbf{H}$. Therefore, the mean curvature motion provides a flow that computes (local) minimal surfaces [8]. Computing the Euler-Lagrange of A_R, we get

$$\mathcal{S}_t = (g\mathbf{H} - \nabla g \cdot \mathcal{N})\mathcal{N}. \tag{3}$$

This is the basic weighted minimal surface flow. Taking a level set representation, the steepest descent method to minimize (2), yields

$$\frac{\partial u}{\partial t} = |\nabla u|\mathrm{div}\left(g(I)\frac{\nabla u}{|\nabla u|}\right) = g(I)|\nabla u|\mathrm{div}\left(\frac{\nabla u}{|\nabla u|}\right) + \nabla g(I)\cdot\nabla u. \tag{4}$$

We note that comparing with previous geometric surface evolution approaches for $3D$ object detection, the minimal surfaces model includes a new term, $\nabla g\cdot\nabla u$. This term is fundamental for detecting boundaries with fluctuations in their gradient; see [5] for details.

As in the $2D$ case, we can add a constant force to the minimization problem (minimizing volume), obtaining the general *minimal surfaces model* for object detection:

$$\frac{\partial u}{\partial t} = |\nabla u|\mathrm{div}\left(g(I)\frac{\nabla u}{|\nabla u|}\right) + \nu g(I)|\nabla u|. \tag{5}$$

This is the flow we will further analyze and use for $3D$ object detection. It has the same properties and geometric characteristics as the geodesic active contours, leading to accurate numerical implementations and topology free object segmentation. The following results can be proved for this flow

Theorem 1 ([6]). *Assume that $g \geq 0$ is sufficiently smooth. Then, for any Lipschitz initial condition u_0, there exists a unique viscosity solution $u(t,x)$ of (5) with $u(0,x) = u_0(x)$.*

In practice, we choose an initial condition u_0 with $\{x : u_0(x) \leq 0\}$ containing the desired object and we let it evolve according to (5). The active surface $\mathcal{S}(t)$ is the boundary of the set $\{x : u(t,x) \leq 0\}$. One can show [6] the independence of the evolution from the particular function u_0 used to define the initial active surface. Finally, the model (5) enables us to show the correctness of the geometric formulation in some special yet important cases. We have

Theorem 2 ([6]). *Assume that $\mathcal{S} = \{x : g(x) = 0\}$ is a compact connected smooth surface embedded in $\mathbb{R}^3$ which is unknotted. Then, if the constant ν is sufficiently large, then $\mathcal{S}(t) \rightarrow \mathcal{S}$ in the Hausdorff distance as $t \rightarrow \infty$. The same result can be proved for all compact smooth surfaces which can be unknotted by adding them a finite number of handles. And also for finite unions of surfaces in that class.*

This covers a large class of surfaces which can be found in practice. Several questions arise concerning this theorem: 1- how large should the constant ν be? It can be seen from the proof in [6] that ν should be larger than the mean curvature of the evolving surfaces. A reasonable assumption is that ν should be larger than the curvature of the desired surface. On the other hand, for initial condition of a surface close to the desired object, one can choose $\nu = 0$. In practice, convergence can also be obtained for $\nu = 0$ if obstacles do not stop the active surface, yet the process is slower. 2- The presence of noise may disturb the convergence. This can be avoided by preprocessing the original image I. In practice, if the noise is not dominant and is not structured along a surface, it will not stop the active surface. 3- The above theorem assumes that the desired surface is given by $g(x) = 0$. We do not give a proof for the general case in which $g(x) > 0$ along the desired surface. In that case the equilibrium position should be along the local minimum and a balance of the forces yields the result.

In [13] it was shown that the curvature along the $2D$ geodesics minimizing the weighted arclength may be bounded by $|\kappa| \leq \sup_{p\in[0,a]\times[0,b]} \left\{ \frac{|\nabla g(I(p))|}{g(I(p))} \right\}$. This result is obtained directly form the Euler-Lagrange equation of the weighted arclength integral. It is easy to see that there is no need for the geodesic itself for limiting the curvature values. In [13], motivated by [21, 22], this bound helped in the construction of different potential functions.

A straightforward generalization of this result to our three dimensional model yields the bound over the mean curvature $\mathbf{H}$. From the equations above, it is clear that for a steady state (*i.e.* $\mathcal{S}_t = 0$) the mean curvature along the surface $\mathcal{S}$ is given by $\mathbf{H} = \frac{\nabla g \cdot \mathcal{N}}{g} - \nu$. We readily obtain the following upper bound for the mean curvature magnitude along the final surface $|\mathbf{H}| \leq \sup \left\{ \frac{|\nabla g|}{g} \right\} + |\nu|$, where the sup operation is taken over all the $3D$ domain. The above bound gives an estimation of the allowed gaps in the edges of the object to be detected as a function of ν. A pure gap is defined as a part of the object boundary at which, for some reason, g =constant$\neq 0$ in a large enough neighborhood. At these locations $|\mathbf{H}| = |\nu|$. Therefore, pure gaps of radius larger than $1/\nu$ will cause the propagating surface to penetrate into the segmented object. It is also clear that

$\nu = 0$ allows the detection of gaps of any given size, and the boundary at such places will be detected as the minimal surface 'gluing' the gaps boundaries.

The basic equations for $3D$ segmentation here described, and those for $2D$ in [5], were recently independently proposed by Kichenassamy *et al.* [18, 19] based on a slightly different initial approach. Shah [33] also recently presented a $2D$ active contours formulation as the one in [5], which is the $2D$ analogue of the model here described. Although the works in [18, 33] also present the problem of $2D$ active contours as geodesic computations, they do not show the connections between energy models and curve evolution ones. Actually, to the best of our knowledge, non of the previous works on curve/surface evolution for object segmentation show the mathematical relation between those models and classical energy approaches, as done in [5] for the $2D$ case and extended in this paper and in [6] for the $3D$ one. Actually, in general the two approaches are considered independent. In [5, 6] and here we show that they are mathematically connected, and one can enjoy the advantages of both of them in the same model. Although the extension from the $2D$ model to the $3D$ one is easy, no $3D$ examples are presented in [18, 33]. Also, not all the theoretical results here quoted [6] can be found in [18, 19, 33] (in [19] the authors do show a number of very important theoretical results as those in [6] and quoted here). Three dimensional examples are given in [37], where similar equations as the presented are proposed. The equations there are obtained by extending the flows in [4, 23], again without showing that they can be obtained in a natural fashion from a re-interpretation of energy based snakes via minimal surfaces. In [35], motivated by work reported in [20], the authors based their work on the models in [4, 23]. One of the key ideas there, motivated by the shape theory of shocks developed by Kimia *et al.*, is to perform multiple initializations. A normalized version of A was derived in [14] from a different point of view, giving as well different flows for $2D$ active contours. Extension of that model to $3D$ was presented in [12].

4 Experimental results

We now present some examples of our minimal surfaces deformable model (5). The numerical implementation is based on the algorithm for surface evolution via level sets [26]. It allows the evolving surface to change topology without monitoring the deformation. Using new results in [1], the algorithm can be made to converge very fast. In the numerical implementation of Eq. (5) we have chosen central difference approximation in space and forward difference approximation in time. This simple selection is possible due to the stable nature of the equation, however, when the coefficient ν is taken to be of high value or when the gradient term is dominant, more sophisticated approximations are required [26].

In our examples, the initialization is in general given by a surface surrounding all the possible objects in the scene. In the case of outward flows [5], a surface is initialized inside each object. The first example of the minimal surfaces deformable model is presented in Figure 1. A 'knotted surface' composed of two tori forming a 'chain' is detected. The initial surface is an ellipsoid surrounding

the two tori (top left). Note how the model manages to change its topology and detect the final surface (bottom right).

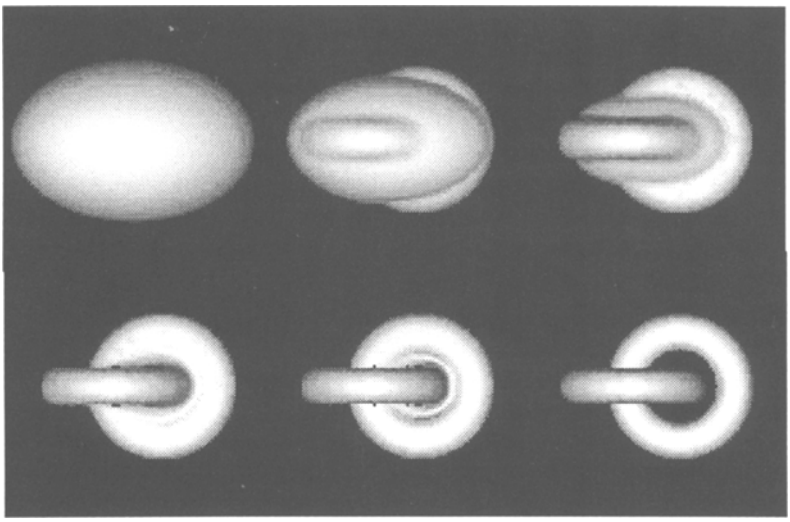

Fig. 1. Detection of two linked tori.

Figure 2 presents the $3D$ detection of a tumor in an MRI image. The initial surface is presented in the first row on the left followed by 3 evolution steps. The final surface, the 'weighted minimal surface', is presented at the lower right frame. Figure 3 shows slices of the $3D$ detection painted on the corresponding MRI data.

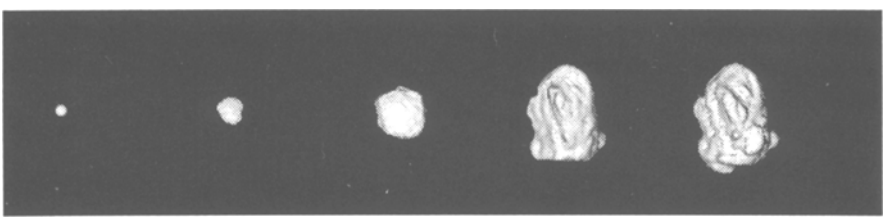

Fig. 2. Detection of a tumor in MRI.

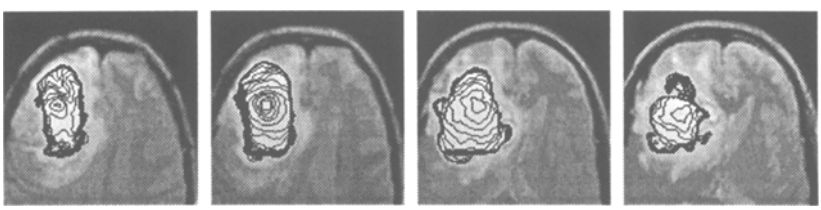

Fig. 3. Slices of the $3D$ detection in Figure 2.

Figure 4 presents the segmentation of the interior and exterior of a $3D$ MRI data of a bone. The two slices show the process of locating the outer and inner parts. Two views of the final segmentation of the inner and outer parts are presented in upper and lower rows. This figure also demonstrate the power of the the proposed technique in accurate analysis of medical images.

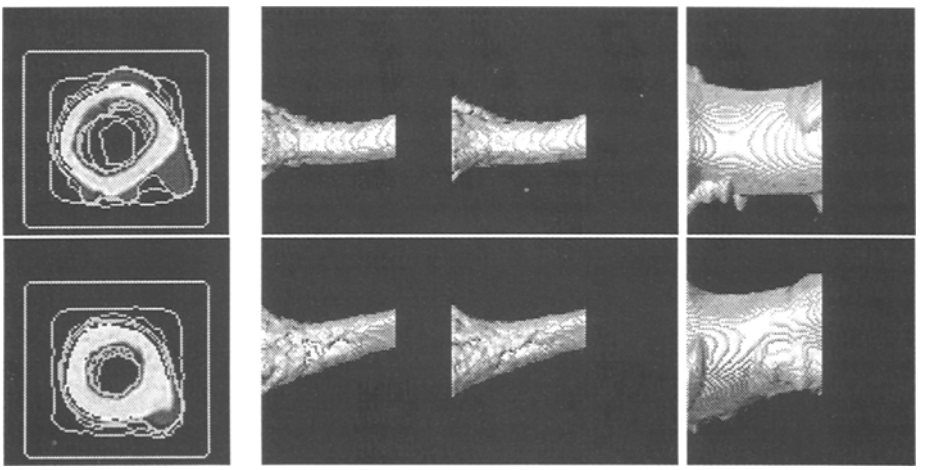

Fig. 4. Two slices and two orthographic views of $3D$ detection of the inner and outer parts of a bone in an MRI image.

5 Concluding remarks

In this paper we presented a novel formulation of deformable surfaces for $3D$ object detection, extending our previous $2D$ work [5]. We proposed a solution to deformable surfaces approach for boundary detection. It is given as a minimal surface in a Riemannian space defined by a metric derived from the given image. This means that detecting the object is equivalent to finding a surface of minimal weighted area. This approach allowed to relate classical energy based models with new surface evolution ones. The minimal surfaces formulation introduced a new term that attracts the deforming surface to the boundary, improving the detection of boundaries with large differences in their gradient. This new term also frees the model from the need to estimate critical parameters. Therefore, the minimal surfaces formulation not only connects previous models, but also improves them. Results regarding existence, uniqueness, stability, and correctness of the solution obtained by our model were summarized and will be reported elsewhere.

Experiments for different kind of images were presented. These experiments demonstrate the ability to detect several objects, as well as the power to simultaneously detect interior and exterior boundaries. The sub-pixel accuracy intrinsic

to the algorithm allows to perform accurate measurements after the object is detected [28].

Acknowledgments
The authors thank Prof. J. Blat, Prof. P.L. Lions, and Prof. J.M. Morel for interesting discussions and their constant support. The work of RK was partially supported by the Applied Mathematical Science subprogram of the Office of Energy Research, U.S. Department of Energy, under Contract Number DE-AC03-76SF00098.

References

1. D. Adalsteinsson and J. A. Sethian, "A fast level set method for propagating interfaces," *J. of Comp. Phys.*, **118**:269–277, 1995.
2. L. Alvarez, F. Guichard, P. L. Lions, and J. M. Morel, "Axioms and fundamental equations of image processing," *Arch. Rational Mechanics* **123**, 1993.
3. A. Blake and A. Zisserman, *Visual Reconstruction*, MIT Press, Cambridge, 1987.
4. V. Caselles, F. Catte, T. Coll, F. Dibos, "A geometric model for active contours," *Numerische Mathematik* **66**, pp. 1-31, 1993.
5. V. Caselles, R. Kimmel, and G. Sapiro, "Geodesic active contours," to appear *International Journal of Computer Vision*. A short version appears at *ICCV'95*, Cambridge, June 1995.
6. V. Caselles, R. Kimmel, G. Sapiro and C. Sbert, "Minimal surfaces: A three-dimensional segmentation approach," *Technion Technical Report* **973**, June 1995.
7. V. Caselles and C. Sbert, "What is the best causal scale-space for 3D images?," *SIAM J. on Applied Math*, to appear.
8. D. Chopp, "Computing minimal surfaces via level set curvature flows," *J. of Comp. Phys.*, 106(1):77–91, 1993.
9. P. Cinquin, "Un modele pour la representation d'images medicales 3d," *Proc. Euromedicine, Sauramps Medical*, **86**, pp 57-61, 1986.
10. L. D. Cohen, "On active contour models and balloons," *CVGIP: Image Understanding* **53**, pp. 211-218, 1991.
11. I. Cohen, L. D. Cohen, and N. Ayache, "Using deformable surfaces to segment 3D images and infer differential structure," *CVGIP: Image Understanding* **56**, pp. 242-263, 1992.
12. L. D. Cohen and I. Cohen, "Finite element methods for active contour models and ballons for 2D and 3D images," *IEEE Tran. on PAMI* **15**(11), November, 1993.
13. L. D. Cohen, and R. Kimmel, "Minimal geodesics of active contour models for edge integration and segmentation," TR-INRIA, 1995.
14. P. Fua and Y. G. Leclerc, "Model driven edge detection," *Machine Vision and Applications*, **3**, pp. 45-56, 1990.
15. M. Gage and R. S. Hamilton, "The heat equation shrinking convex plane curves," *J. Differential Geometry* **23**, pp. 69-96, 1986.
16. M. Grayson, "The heat equation shrinks embedded plane curves to round points," *J. Differential Geometry* **26**, pp. 285-314, 1987.
17. M. Kass, A. Witkin, and D. Terzopoulos, "Snakes: Active contour models," *International Journal of Computer Vision* **1**, pp. 321-331, 1988.
18. S. Kichenassamy, A. Kumar, P.Olver, A. Tannenbaum, and A. Yezzi, "Gradient flows and geometric active contour models," *Proc. ICCV*, Cambridge, June 1995.

19. S. Kichenassamy, A. Kumar, P.Olver, A. Tannenbaum, and A. Yezzi, "Conformal curvature flows: from phase transitions to active vision," to appear *Archive for Rational Mechanics and Analysis.*
20. B. B. Kimia, A. Tannenbaum, and S. W. Zucker, "Shapes, shocks, and deformations, I," *International Journal of Computer Vision* **15**, pp. 189-224, 1995.
21. R. Kimmel, A. Amir, A. M. Bruckstein, "Finding shortest paths on surfaces using level sets propagation," *IEEE–PAMI*, 17(6):635–640, 1995.
22. R. Kimmel, N. Kiryati, A. M. Bruckstein, "Distance maps and weighted distance transforms," *Journal of Mathematical Imaging and Vision,* Special Issue on Topology and Geometry in Computer Vision, to appear.
23. R. Malladi, J. A. Sethian and B. C. Vemuri, "Shape modeling with front propagation: A level set approach," *IEEE Trans. on PAMI,* January 1995.
24. T. McInerney and D. Terzopoulos, "Topologically adaptable snakes," *Proc. ICCV*, Cambridge, June 1995.
25. P. J. Olver, G. Sapiro, and A. Tannenbaum, "Invariant geometric evolutions of surfaces and volumetric smoothing," *SIAM J. of Appl. Math.*, to appear.
26. S. J. Osher and J. A. Sethian, "Fronts propagation with curvature dependent speed: Algorithms based on Hamilton-Jacobi formulations," *Journal of Computational Physics* **79**, pp. 12-49, 1988.
27. R. Osserman, *Survey of Minimal Surfaces*, Dover, 1986.
28. G. Sapiro, R. Kimmel, and V. Caselles, "Object detection and measurements in medical images via geodesic active contours," SPIE-Vision Geometry, San Diego, July 1995.
29. G. Sapiro, R. Kimmel, D. Shaked, B. B. Kimia, and A. M. Bruckstein, "Implementing continuous-scale morphology via curve evolution," *Pattern Recog.* **26:9**, pp. 1363-1372, 1993.
30. G. Sapiro and A. Tannenbaum, "On affine plane curve evolution," *Journal of Functional Analysis* **119:1**, pp. 79-120, 1994.
31. G. Sapiro and A. Tannenbaum, "Affine invariant scale-space," *International Journal of Computer Vision* **11:1**, pp. 25-44, 1993.
32. H.M. Soner, "Motion of a set by the curvature of its boundary," *J. of Diff. Equations* **101**, pp. 313-372, 1993.
33. J. Shah, "Recovery of shapes by evolution of zero-crossings," Technical Report, Math. Dept. Northeastern Univ. Boston MA, 1995.
34. R. Szeliski, D. Tonnesen, and D. Terzopoulos, "Modeling surfaces of arbitrary topology with dynamic particles," *Proc. CVPR*, pp. 82-87, 1993.
35. H. Tek and B. B. Kimia, "Image segmentation by reaction-diffusion bubbles," *Proc. ICCV*, Cambridge, June 1995.
36. D. Terzopoulos, A. Witkin, and M. Kass, "Constraints on deformable models: Recovering 3D shape and nonrigid motions," *Artificial Intelligence* **36**, pp. 91-123, 1988.
37. R. T. Whitaker, "Volumetric deformable models: Active blobs," *ECRC TR* **94-25**, 1994.
38. R. T. Whitaker, "Algorithms for implicit deformable models," *Proc. ICCV'95*, Cambridge, June 1995.
39. S. C. Zhu, T. S. Lee, and A. L. Yuille, "Region competition: Unifying snakes, region growing, energy/Bayes/MDL for multi-band image segmentation," *Proc. ICCV*, Cambridge, June 1995.